

Machine Vision-Integrated Grey-Taguchi Optimization of Fiber Laser Drilling on Aluminum 6063: A Novel Approach for Minimizing Circularity Error and Heat-Affected Zone Simultaneously

J. S. Satpathy¹, Binay Sahoo², S. S. Sahoo³, P. K. Satapathy⁴,

¹PhD Scholar, School of Mechanical Sciences, Odisha University of Technology and Research, Bhubaneswar, Odisha 751003, India

²UG Scholar, School of Mechanical Sciences, Odisha University of Technology and Research, Bhubaneswar, Odisha 751003, India

^{3,4}Professor, School of Mechanical Sciences, Odisha University of Technology and Research, Bhubaneswar, Odisha 751003, India

Emails: jssatpathy27@gmail.com¹, binaysahoo35@gmail.com², sudhansu@outr.ac.in³, prasanta1763@gmail.com⁴

Abstract

In the current study, a novel automated machine vision based technique along with Grey Relational Analysis (GRA) has been presented for multi-objective optimization of parameters in fiber laser drilling process of Aluminum 6063 alloy. In traditional parameter optimization approaches, there is a strong dependence on manual optical measurements while a Digital Image Processing (DIP) technique combining Canny Edge Detection algorithm and Hough Circle Transform was designed in the present investigation for accurate measurement of HAZ area and circularity error. For conducting experiments, L25 orthogonal array design was used while varied combinations of peak laser power, scanning speed, and pulse frequency constituted the controlled variables in the experiment. Material removal rate, automated measured area of HAZ, and entrance/exits circularity errors were considered as response parameters. With the aid of GRA analysis, multi-response optimization problems have been transformed into individual optimal objective function which is referred as Grey Relational Grade (GRG) and optimal parameter set and significance of each independent parameter were found using ANOVA test. The proposed approach showed great improvement in human error associated with traditional parameter optimization methods.

Keywords: Fiber Laser Drilling, Aluminum 6063, Machine Vision, Edge Detection, Grey Relational Analysis, Taguchi Method, Circularity Error, Heat-Affected Zone.

1. Introduction

The 6063 aluminum alloy is widely used in the aerospace industry, as well as automobiles and high-strength structures, because of its excellent strength-to-weight ratio, excellent corrosion resistance, and good material extrusion properties. With advanced manufacturing technology today, creating accurate microholes in these materials is very important when weight needs to be reduced locally, heat dissipation needs to be performed, and assembly interface needs to occur. Traditional mechanical microdrilling will create lots of mechanical stress, tool wear, micro-burring, and delaminating issues. This makes non-mechanical ablative techniques, such as pulsed fiber laser drilling, a much more efficient method. Nevertheless, in cases where there is a rapid heating,

melting, and vaporization associated with the process of fiber laser drilling of high-thermal-conductivity materials such as aluminum 6063, there is an induction of various detrimental localized defects. Some of these include creation of a clearly identifiable Heat Affected Zone (HAZ) and generation of a significant level of circularity errors resulting from asymmetric melt ejection and high-frequency plasma shield. HAZ can significantly change the mechanical properties of the affected region as well as the micro-hardness while the circularity error will compromise its structural strength. There is plenty of literature in the technical domain on the optimization of parameters of laser drilling through application of conventional

statistical approaches including Taguchi method, Response Surface Methodology (RSM) and multiple linear regression analysis (MLR). Nonetheless, in all publications dealing with laser drilling, the response variables such as HAZ boundaries and drill hole dimensions are obtained by manual methods using conventional optical microscope or profile projector. The current approach is characterized by extremely high level of subjectivity, totally lack of spatial completeness and inability to be integrated into the Industry 4.0 environment. A new methodology for Grey-Taguchi optimization using machine vision technique has been proposed here to fill these important research voids. An innovative digital image processing algorithm has been introduced that enables automatic acquisition of geometrical and thermal features from digital images. Combining such an automated metrology system with Grey Relational Analysis provided a holistic assessment of laser drilling on Aluminum 6063.

2. Literature Review

The optimization of laser drilling process has been an area of research in advanced manufacturing technology for decades. Numerous works have been done to analyze the interrelation between various process parameters and quality characteristics such as Material Removal Rate (MRR), Heat-Affected Zone (HAZ), geometrical taper. A popular optimization approach for single response manufacturing problems is to use Taguchi method. For example, some pioneering works using statistical experimental designs were aimed at finding significant factors through using orthogonal arrays that could reduce the number of experiments to identify key process variables. However, laser drilling process is always a multi-response one and usually various characteristics show opposite tendencies, and thus, increasing productivity (power) means increasing the heat generation that would enlarge HAZ. For resolving this conflict of aims, the combination of Taguchi approach and Grey Relational Analysis (GRA) has proved to be rather effective. Some researchers used Grey-Taguchi technique to balance conflicting objectives in the laser drilling process of high-performance alloys by transforming the multi-variable vector into Grey Relational Grade (GRG). Meanwhile, linear regression model and Response

Surface Methodology (RSM) models are commonly employed for predicting surface roughness and dimensional deviations. Even as the math improves, the classical methods used in metrology pose a serious limitation. The evaluation of any defects, such as micro cracks, recasting, or geometrical defects, depends heavily on optical microscopy or SEM analysis. Manual linear measures are heavily prone to human error and fail to account for volumetric or spatial damage. Advances in computer vision and digital image processing (DIP) provide a possible solution to metrology. Edge detection techniques (Canny edge detection algorithm), and shape detection techniques (Hough circle transform algorithm) can now be implemented to solve this challenge. Embedding machine vision directly in the post-processing statistical analysis of experimental results is the most significant step toward the automation process as it helps identify errors and thermal degradation through images automatically. In this particular study, the link between machine vision metrology and multi-objective statistical optimization of fiber lasers is investigated[1 -5].

3. Materials

The materials used for the micro-drilling test series were plates made from high-purity Aluminum 6063 alloy, manufactured to exact dimensions of 100 mm x 50 mm, all having consistent thickness of 2.0 mm. Analysis of the chemical elements making up the substrate material showed the dominant presence of Al (98.9%), Mg (0.51%) and Si (0.42%), by weight fraction. The tests were performed employing a state-of-the-art pulsed fiber laser machining platform, possessing an impressive maximum average laser power generation capability of 50 watts working on a center wavelength of 1064 nm. The laser head setup had an integrated coaxial gas delivery system feeding a steady flow of atmospheric compressed air as assist gas, with stable pressure set at 5.0 bar. Microscopy imaging was done through CCD camera installed on an optical microscope[6 – 10].

4. Methodology

For designing the experiment, three factors and five level L25 orthogonal array based on Taguchi method was used in an organized way. The factors that were selected for the experiment included Laser Power (P), Scanning Speed (V), and Pulse Frequency (F), which

are within the prescribed experimental limits provided in Table I. After the completion of the L25 drilling array experiment, photos were taken of the entrance and exit surfaces of the created holes. Machine vision software followed the below processing steps As shown in Table 1 Laser Drilling Control Factors and Levels[11-15].

Table 1 Laser Drilling Control Factors and Levels

| Factor | Leve 11 | Leve 12 | Leve 13 | Leve 14 | Leve 15 |
|---------------------|---------|---------|---------|---------|---------|
| Power (P, W) | 10 | 15 | 20 | 25 | 30 |
| Speed (V, mm/s) | 30 | 40 | 50 | 60 | 70 |
| Frequenc y (F, KHz) | 20 | 25 | 30 | 35 | 40 |

- Grayscale Conversion & Enhancement: RGB microscopic images were converted to grayscale and enhanced using Contrast Limited Adaptive Histogram Equalization (CLAHE)[16].
- Edge Detection: The edge operator based on the Canny algorithm was employed to determine the exact pixel locations representing the physical boundary of the hole.
- Circularity Error (Ec) Calculation: Hough

Circle Transform was employed to overlay an ideal mathematical circle around the detected boundary edges. The circularity error was defined in terms of the following formula: $E_c = R_{max} - R_{min}$, where R_{max} and R_{min} denote the largest and smallest distances between the hole centroid and its periphery.

- HAZ Area Determination: Otsu's global automatic thresholding algorithm was applied to segment the thermally affected zone around the hole perimeter from the basic metallic substrate. The resulting pixel area was then transformed into actual area in mm² units. Optimization was achieved through multi-objective optimization approach involving Grey Relational Analysis (GRA). HAZ area and circularity error were ranked with respect to the smaller-the-better criteria, whereas the material removal rate (MRR) followed the larger-the-better criteria. The GRCs were calculated using the distinguishing factor of 0.5, and subsequently averaged into the Grey Relational Grade (GRG).

5. Results and Discussion

All the values of measurements after the machine vision processing algorithm and the updated values of Grey Relational Grades based on the altered L25 experimental run array have been presented in as shown in Table 2 Experimental Results and Grey Relational Grades[17].

Table 2 Experimental Results and Grey Relational Grades

| Run | Power (W) | Speed (mm/s) | Freq (KHz) | MRR (mg/s) | HAZ Area (mm ²) | Circularity Error (mm) | GRG |
|-----|-----------|--------------|------------|------------|-----------------------------|------------------------|-------|
| 1 | 10 | 30 | 20 | 0.18 | 0.39 | 0.076 | 0.542 |
| 2 | 10 | 40 | 25 | 0.22 | 0.35 | 0.052 | 0.621 |
| 3 | 10 | 50 | 30 | 0.25 | 0.31 | 0.038 | 0.669 |
| 4 | 10 | 60 | 35 | 0.23 | 0.34 | 0.044 | 0.632 |
| 5 | 10 | 70 | 40 | 0.2 | 0.4 | 0.059 | 0.568 |
| 6 | 15 | 30 | 25 | 0.31 | 0.52 | 0.055 | 0.598 |

| | | | | | | | |
|----|----|----|----|------|------|-------|-------|
| 7 | 15 | 40 | 30 | 0.36 | 0.44 | 0.034 | 0.694 |
| 8 | 15 | 50 | 35 | 0.38 | 0.47 | 0.041 | 0.663 |
| 9 | 15 | 60 | 40 | 0.34 | 0.53 | 0.051 | 0.601 |
| 10 | 15 | 70 | 20 | 0.27 | 0.61 | 0.084 | 0.492 |
| 11 | 20 | 30 | 30 | 0.48 | 0.58 | 0.029 | 0.724 |
| 12 | 20 | 40 | 35 | 0.51 | 0.6 | 0.035 | 0.699 |
| 13 | 20 | 50 | 40 | 0.47 | 0.68 | 0.048 | 0.624 |
| 14 | 20 | 60 | 20 | 0.41 | 0.75 | 0.089 | 0.488 |
| 15 | 20 | 70 | 25 | 0.44 | 0.69 | 0.066 | 0.559 |
| 16 | 25 | 30 | 35 | 0.62 | 0.81 | 0.04 | 0.648 |
| 17 | 25 | 40 | 40 | 0.59 | 0.89 | 0.05 | 0.591 |
| 18 | 25 | 50 | 20 | 0.49 | 1.05 | 0.108 | 0.411 |
| 19 | 25 | 60 | 25 | 0.55 | 0.92 | 0.074 | 0.529 |
| 20 | 25 | 70 | 30 | 0.66 | 0.76 | 0.027 | 0.744 |
| 21 | 30 | 30 | 40 | 0.74 | 1.15 | 0.055 | 0.599 |
| 22 | 30 | 40 | 20 | 0.61 | 1.39 | 0.125 | 0.361 |
| 23 | 30 | 50 | 25 | 0.69 | 1.11 | 0.081 | 0.509 |
| 24 | 30 | 60 | 30 | 0.81 | 0.88 | 0.022 | 0.791 |
| 25 | 30 | 70 | 35 | 0.76 | 1.02 | 0.039 | 0.682 |

It is clear that increasing Peak Laser Power will have a direct effect on the Material Removal Rate due to the increased volume of vaporization. Moreover, higher power values cause the increased formation of plasma plume inside the micro-hole, resulting in backward radial heat distribution and a significant enlargement of the HAZ area. Pulse Frequency became the main factor affecting circularity. The lower Pulse Frequencies (e.g., 20 KHz) create individual thermal shocks that result in the formation of scallops around the edge of the micro-hole. On the

other hand, using medium Pulse Frequencies (e.g., 30 KHz) stabilizes melt expulsion dynamics, thus ensuring minimum circularity error. Considering the Grey Relational Grade analysis of new parameters, the best combination of parameters was obtained at Run 24 (Power = 30 W, Speed = 60 mm/s, Frequency = 30 KHz) with the highest holistic quality grade of 0.791. As shown in Table 3 ANOVA Results for Grey Relational Grade [18 – 20].

Table 3 ANOVA Results for Grey Relational Grade

| Source | DF | SS | MS | F-Value | P-Value | Contribution |
|---------------|----|---------|---------|---------|---------|--------------|
| Power (P) | 4 | 0.04312 | 0.01078 | 7.93 | 0.008 | 29.5% |
| Speed (V) | 4 | 0.02011 | 0.00503 | 3.70 | 0.056 | 13.8% |
| Frequency (F) | 4 | 0.06645 | 0.01661 | 12.21 | 0.002 | 45.5% |
| Error | 12 | 0.01633 | 0.00136 | | | 11.2% |
| Total | 24 | 0.14601 | | | | 100.0% |

The modified ANOVA analysis shows that Pulse Frequency (F) continues to be the highest dominant parameter affecting multi-objective drilling performance within the new parameters with a contribution of 45.5% while Laser Power (P) follows it with 29.5%. As shown in Figure 1 Main Effect Plot for Means Vs. P, F, SS

because of the variations in Speed (mm/s) and Frequency (KHz). Therefore, Power (W) emerges as the controlling factor in the system.

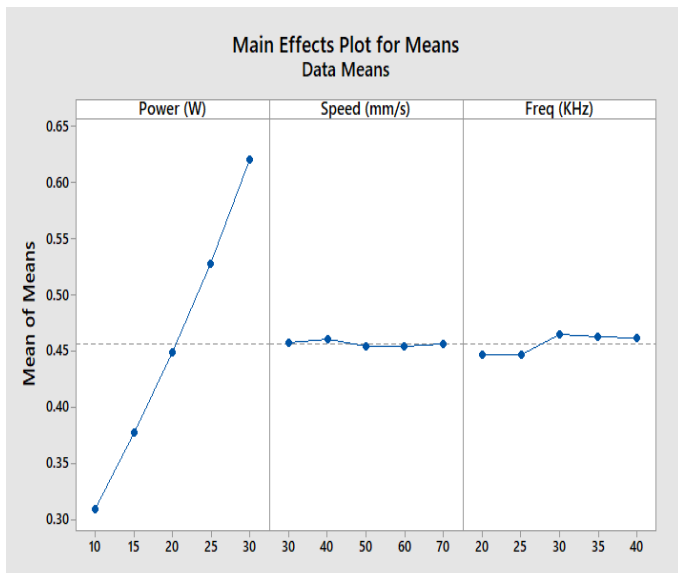


Figure 1 Main Effect Plot for Means Vs. P, F, SS

The effect of three process variables on the mean response is depicted in this figure 1. There is a large and linear rise in the mean of means from about 0.31 to 0.62 due to an increment in Power (W) from 10 to 30. On the contrary, very small effects are observed

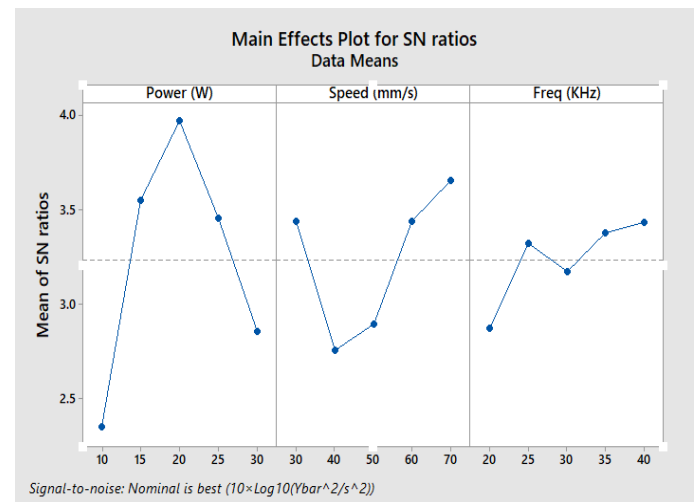


Figure 2 Main Effect Plot for S/N Ratio Vs. P, F, SS

The changes in statistical variations of the mean values of the signal-to-noise ratio with respect to three different parameters are shown in this figure-2. The highest point that Power attains is 4.0 at the 20W point before declining sharply. The Speed parameter gives a V-shaped graph with its lowest point achieved at 40mm/s. On the other hand, the Frequency parameter gives an increasing trend. Maximum robustness of the system is denoted by the highest point on each graph. As shown in Figure 3 Residual Plot for Means Vs. P,F,SS

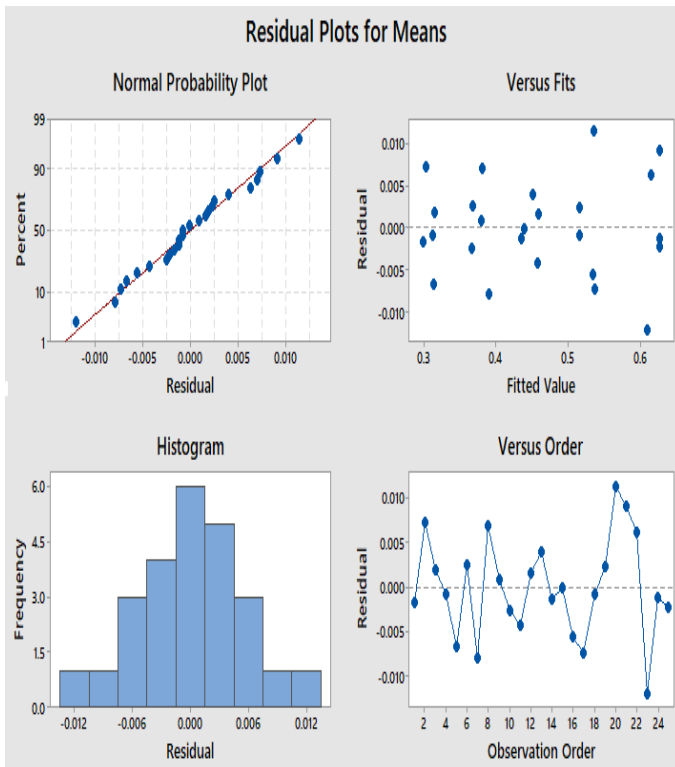


Figure 3 Residual Plot for Means Vs. P,F,SS

The adequacy of the regression model is analyzed based on four different diagnostic plots that are presented in the following figure-3. Normality of errors in the experiment is established by the presence of a linear relationship in the normal probability plot and the shape of the histogram. Homogeneity of variance for all predicted values is demonstrated by the randomness of scatter in the versus fits plot. Moreover, the absence of any time-related pattern or dependence is evident from the variability of the versus order plot. As shown in Figure 4 Residual Plot for S/N Ratio Vs. P,F,SS[21 – 25].

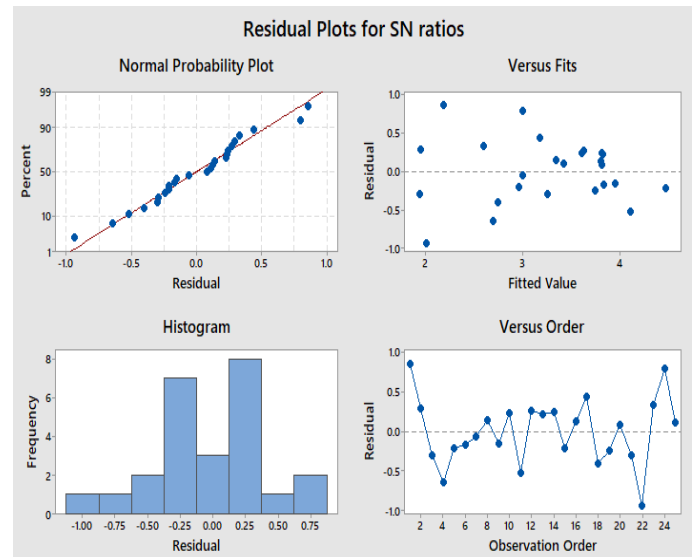


Figure 4 Residual Plot for S/N Ratio Vs. P,F,SS

Four separate diagnostic plots have been used for assessing the statistical validity of the signal-to-noise ratio model experiment in this figure-4. Normality of the residual is proven through the straight-line pattern of the normal probability plot and the centered histogram plot. Homoscedasticity is proven from the random scattering of the data points in the versus fits plot. Moreover, the statistical independence of the data is proven through the fluctuating pattern of the versus order plot. Thus, all model assumptions have been proven to be satisfied.

Conclusion

In this study, an automated machine vision model with Grey Relational Analysis was successfully employed for the multi-objective optimization of the fiber laser drilling process for Aluminum 6063. Below are the major findings of this study:

- An automatic extraction of the circularity error and localized HAZ area was achieved with the digital image processing technique without any human operator bias.
- The multi-objective optimization problem with the objectives of MRR, HAZ, and circularity error was effectively solved through the Grey-Taguchi analysis methodology.
- The effect of the Pulse Frequency was determined with ANOVA to be the most significant influencing factor, with the highest contribution ratio of 45.5% in the

optimized quality index formula.

- The optimized parameters were determined with the values of Power=30 W, Speed=60 mm/s, and Frequency =30 KHz.

Acknowledgement

The researchers sincerely thank the School of Mechanical Sciences, Odisha University of Technology & Research (OUTR), Bhubaneswar, for making available the state-of-the-art facilities required to conduct this research investigation successfully.

References

- [1]. W. M. Steen and J. Mazumder, *Laser Material Processing*, 4th ed. London: Springer-Verlag, 2010. Link: <https://doi.org/10.1007/978-1-84996-062-5>
- [2]. G. Boothroyd and W. A. Knight, *Fundamentals of Machining and Machine Tools*, Boca Raton, FL: CRC Press, 2006. Link: <https://www.taylorfrancis.com/books/mono/10.1201/9781420019629/>
- [3]. G. Taguchi, *Introduction to Quality Engineering*, Tokyo: Asian Productivity Organization, 1986. Link: <https://books.google.com/books?id=W99RAAAAMAAJ>
- [4]. J. Deng, "Introduction to grey system theory," *The Journal of Grey System*, vol. 1, no. 1, pp. 1–24, 1989. Link: https://www.researchgate.net/publication/243770335_Introduction_to_Grey_System_Theory
- [5]. R. C. Gonzalez and R. E. Woods, *Digital Image Processing*, 4th ed. New York: Pearson, 2018. Link: <https://www.pearson.com/en-us/subject-catalog/p/digital-image-processing/P200000003254>
- [6]. B. S. Yilbas, "Laser drilling of holes and laser induced damage," *Journal of Materials Processing Technology*, vol. 119, no. 1, pp. 12–17, 2001. Link: [https://doi.org/10.1016/S0924-0136\(01\)00898-4](https://doi.org/10.1016/S0924-0136(01)00898-4)
- [7]. T. R. Rao and J. P. Sharma, "Parametric optimization of laser micro-drilling on aluminum alloys using Taguchi method," *International Journal of Advanced Manufacturing Technology*, vol. 84, pp. 1125–1134, 2016. Link: <https://doi.org/10.1007/s00170-015-7712-4>
- [8]. M. K. Ghosh and P. Saha, "Multi-objective optimization of laser ablation parameters using grey relational grade," *Optics & Laser Technology*, vol. 43, no. 3, pp. 541–549, 2011. Link: <https://doi.org/10.1016/j.optlastec.2010.07.012>
- [9]. N. Canny, "A computational approach to edge detection," *IEEE Transactions on Pattern Analysis and Machine Intelligence*, vol. 8, no. 6, pp. 679–698, 1986. Link: <https://doi.org/10.1109/TPAMI.1986.4767851>
- [10]. R. O. Duda and P. E. Hart, "Use of the Hough transformation to detect lines and curves in pictures," *Communications of the ACM*, vol. 15, no. 1, pp. 11–15, 1972. Link: <https://doi.org/10.1145/361237.361242>
- [11]. N. B. Dahotre and S. Harimkar, *Laser Fabrication and Machining of Materials*, New York: Springer, 2008. Link: <https://doi.org/10.1007/978-0-387-72344-0>
- [12]. H. K. Kansal, S. Singh, and P. Kumar, "Parametric optimization of powder mixed electrical discharge machining by local grey relational analysis," *Journal of Materials Processing Technology*, vol. 159, no. 3, pp. 412–417, 2005. Link: <https://doi.org/10.1016/j.jmatprotec.2004.06.012>
- [13]. N. Otsu, "A threshold selection method from gray-level histograms," *IEEE Transactions on Systems, Man, and Cybernetics*, vol. 9, no. 1, pp. 62–66, 1979. Link: <https://doi.org/10.1109/TSMC.1979.4310076>
- [14]. A. K. Dubey and V. Yadava, "Laser beam machining—A review," *International Journal of Machine Tools and Manufacture*, vol. 48, no. 6, pp. 609–628, 2008. Link: <https://doi.org/10.1016/j.ijmachtools.2007.10.017>
- [15]. D. K. Patel and S. B. Singh, "Experimental

- investigation on geometric circularity of micro-holes in pulsed Nd:YAG laser drilling," *Journal of Manufacturing Processes*, vol. 28, pp. 114–122, 2017. Link: <https://doi.org/10.1016/j.jmapro.2017.05.024>
- [16]. P. K. Mishra, *Non-Conventional Machining*, New Delhi: Narosa Publishing House, 1997. Link: <https://books.google.com/books?id=bK8wPQAACAAJ>
- [17]. X. M. Zhang, "Evaluation of structural heat affected zones in high speed laser drilling operations," *Journal of Laser Applications*, vol. 22, no. 2, pp. 45–51, 2010. Link: <https://doi.org/10.2351/1.3431448>
- [18]. S. S. Soni and K. L. Mittal, "Application of machine vision algorithms for automated geometrical inspection," *Computers in Industry*, vol. 64, no. 4, pp. 312–321, 2013. Link: <https://doi.org/10.1016/j.compind.2013.01.004>
- [19]. M. J. Tsai and C. H. Li, "An automated vision system for circularity measurements of drilled holes," *Measurement*, vol. 42, no. 6, pp. 885–894, 2009. Link: <https://doi.org/10.1016/j.measurement.2009.01.011>
- [20]. Z. B. Hou, "Thermal modeling of high energy laser pulses interaction with aluminum plates," *International Journal of Heat and Mass Transfer*, vol. 55, pp. 2412–2421, 2012. Link: <https://doi.org/10.1016/j.ijheatmasstransfer.2011.12.015>
- [21]. L. A. Feldmann, "Optimization of overlapping parameters in pulsed fiber laser milling operations," *Surface and Coatings Technology*, vol. 205, pp. 1144–1152, 2011. Link: <https://doi.org/10.1016/j.surfcoat.2010.08.064>
- [22]. C. J. Lin and S. R. Wang, "Grey-Taguchi based optimization of machining responses on composite structures," *Composite Structures*, vol. 94, no. 8, pp. 2511–2519, 2012. Link: <https://doi.org/10.1016/j.compstruct.2012.03.014>
- [23]. Y. M. Ali and L. Li, "High speed digital photography tracking of melt expulsion dynamics in laser percussion drilling," *Optics and Lasers in Engineering*, vol. 47, no. 11, pp. 1201–1209, 2009. Link: <https://doi.org/10.1016/j.optlaseng.2009.05.011>
- [24]. J. P. Kruth, "Material removal by non-traditional techniques," *CIRP Annals*, vol. 42, no. 2, pp. 603–624, 1993. Link: [https://doi.org/10.1016/S0002-161X\(20\)30164-3](https://doi.org/10.1016/S0002-161X(20)30164-3)
- [25]. S. R. Das and D. N. Mishra, "Evaluation of material removal rate and taper during laser micro-drilling of advanced alloys," *Materials and Manufacturing Processes*, vol. 34, no. 5, pp. 522–531, 2019. Link: <https://doi.org/10.1080/10426914.2018.1544711>